Carbon nanotube/zirconia composite-coated separator for a high-performance rechargeable lithium–sulfur battery

Bin Liu, Shan Wang, Xiaomeng Wu, Zhikang Liu, Zhaodongfang Gao, Chuanbin Li, Quanling Yang, Guo-Hua Hu, Chuanxi Xiong

Carbon nanotube/zirconia composite-coated separator for a high-performance rechargeable lithium–sulfur battery

Cite as: AIP Advances **8**, 105315 (2018); https://doi.org/10.1063/1.5044486
Submitted: 13 June 2018 . Accepted: 03 October 2018 . Published Online: 11 October 2018

Bin Liu, Shan Wang, Xiaomeng Wu, Zhikang Liu, Zhaodongfang Gao, Chuanbin Li, Quanling Yang, Guo-Hua Hu, and Chuanxi Xiong

Carbon nanotube/zirconia composite-coated separator for a high-performance rechargeable lithium–sulfur battery

Bin Liu,[1] Shan Wang,[1,a] Xiaomeng Wu,[1] Zhikang Liu,[1] Zhaodongfang Gao,[1] Chuanbin Li,[1] Quanling Yang,[1] Guo-Hua Hu,[2] and Chuanxi Xiong[1,a]
[1]*State Key Laboratory of Silicate Materials for Architectures, School of Materials Science and Engineering, Wuhan University of Technology, Wuhan 430070, China*
[2]*Laboratory of Reactions and Process Engineering (LRGP, CNRS UMR 7274), University of Lorraine–CNRS, 1 rue Grandville, BP 20451, 54001 Nancy, France*

(Received 13 June 2018; accepted 3 October 2018; published online 11 October 2018)

The shuttle effect caused by polysulfides remains a major issue hindering the application of lithium–sulfur (Li-S) batteries. In this work, a composite of organically modified carbon nanotube (CNT) and zirconia (ZrO_2) nanoparticles is synthesized and used as a surface coating on a commercial Celgard separator to restrain the shuttle effect and improve battery performance. Electrolyte uptake and water contact angle measurements show that the CNT/ZrO_2 composite-coated separator has an enhanced electrolyte wettability. Thermal shrinkage results reveal an improvement in the stability of the coated separators, especially at high temperatures. Electrochemical measurements also show the effectiveness of the CNT/ZrO_2 composite-coated separator in a Li–S battery. The initial discharge capacity is improved after coating, as is the capacity retention rate. In addition, a battery with a CNT/ZrO_2 composite-coated separator attains an impressive capacity reversibility as high as 91.7% in a rate performance test from 0.1 to 2 C. The composite coating restrains the shuttle effect effectively and improves the thermal shrinkage properties of the separator. Thus, the use of a CNT/ZrO_2 composite-coated separator should improve the prospects for practical application of Li–S batteries. https://doi.org/10.1063/1.5044486

I. INTRODUCTION

The rapid development and widespread application of portable devices has led to an enormous demand for rechargeable batteries with high energy density.[1] Rechargeable lithium ion batteries are the most promising candidates in this respect.[2] In recent decades, a wide variety of systems with high-capacity anode or cathode materials have been explored, with, for instance, silicon oxycarbide ceramics being considered as novel lithium storage materials[3] and MoS_2–graphene hybrids as electrodes.[4] Owing to their relatively high theoretical mass-specific capacity of 1675 mA·h/g and energy density of 2500 W·h/kg, which are well above those of conventional lithium–graphite batteries, lithium–sulfur (Li–S) batteries have been attracting considerable attention.[5,6] Moreover, sulfur cathodes have the advantages of wide availability of the raw material, cost-effectiveness, and environmental friendliness, making Li–S batteries attractive for industrial applications.

Nevertheless, there remain a number of obstacles to the commercial production of Li–S batteries. One of these is the shuttle effect caused by the solubility of long-chain polysulfide intermediates (Li_2S_x, x = 4, 6, 8) produced during the charge and discharge process, which leads to a loss of active materials and low coulombic efficiency.[7] To address this issue, a variety of approaches have been explored. Effective strategies include tuning the microstructure of the carbon matrix to limit

[a]Corresponding authors. E-mail: cxiong@whut.edu.cn (C. Xiong); shanwang@whut.edu.cn (S. Wang). Phone: +86-027-87387481 (C. Xiong & S. Wang)

polysulfide migration,[8–10] using sulfur copolymers as alternative feedstock for sulfur,[11,12] and retaining long-chain soluble polysulfides in the cathode by the use of various absorbents, such as carbonaceous materials (e.g. carbon nanotubes, graphene, or nanoporous carbon),[13–17] metal oxides,[18,19] and polymer materials.[20,21] However, despite the enhanced electrochemical performance thus achieved, fine control of the phase structure of sulfur composite cathodes usually requires elaborate techniques, which makes it difficult to implement in industrial applications. Therefore, attention has recently turned to approaches involving modifications of the separator.[22–24]

As an indispensable component of liquid electrolyte batteries, the separator is used to prevent physical contact between the anode and cathode, ensuring transport of free ions and meanwhile preventing flow of electrons. Modifications[25] or replacement[26–28] of commercial separators are now major directions of research, including exploration of the mechanisms underlying the operation of separators.[29,30] The porosity, wettability, and thermal shrinkage of separators can influence the specific capacity, cycle life, and security of liquid electrolyte batteries.[31] Previous studies have shown that an electrically conductive coating and metal oxide layer on one side of a separator can accelerate the transport of ions or electrons, enhance absorption of electrolyte, maintain thermal stability, and suppress the shuttle effect of long-chain soluble polysulfides.[23] Because of their high aspect ratios and excellent electrical conductivity, carbon nanotubes have been proposed for the construction of interconnected and conductive networks in Li–S batteries.[32,33] However, virgin carbon nanotubes are always highly entangled and poorly dispersible in solvents, and so there have been few studies focusing on the application of CNT as coatings on separators. Chung and Manthiram[34] adopted a vacuum filtration technique to fabricate a CNT-coated separator, and their results showed that the modified separator endowed the Li–S battery with improved reversible capacity, outstanding electrochemical recovery capability, and prolonged cycle life, although with vacuum filtration there is a risk of separator fracture due to the pressure difference between the top and bottom surfaces. Our previous work has also shown the effectiveness of an organically modified CNT-coated separator in an Li–S battery.[35] As a widely used inorganic oxide, zirconia is attractive because of its chemical and thermal stability, low cost, and nontoxicity, and a zirconia coating layer has already been used in a lithium battery.[36] It should also be noted, however, that polymer-based separators will shrink at high temperatures, leading to safety problems.

In the present study, a novel modified separator is prepared by coating an organically modified CNT and zirconia (ZrO_2) (CNT/ZrO_2) composite onto the surface of a conventional separator. The improvement in electrochemical performance of a lithium sulfur battery incorporating this modified separator is obvious. It is believed that the hydrophilic groups on the organically modified CNT, the ZrO_2, and the porous structure of the composite are all conducive to suppressing the shuttle effect arising from polysulfides, thus improving the cycling performance. In addition, the problem of thermal shrinkage is reduced owing to the thermal stability of the zirconia and CNT. All of these improvements should help pave the way to practical application of Li–S batteries.

II. EXPERIMENTAL

A. Materials

A Celgard 2325 separator was obtained from Celgard LLC. CNT were purchased from Chengdu OC Co., Ltd. Sublimed sulfur, anhydrous ethanol, concentrated HNO_3 (65%), and concentrated H_2SO_4 (98%) were purchased from Shanghai SCR Co., Ltd. Nano-sized zirconium dioxide (ZrO_2), bis(trifluoromethane)sulfonimide lithium (LiTFSI, 98%), 1,2-dimethoxyethane (DME, 99.5%), lithium nitrate ($LiNO_3$, trace metals basis 99.99%), *N*-methyl-2-pyrrolidone (NMP, 99%), and 1,3-dioxolane (DOL, 99.8%) were provided by Aladdin. DC5700 $[(CH_3O)_3Si(CH_2)_3N^+(CH_3)_2(C_{18}H_{37})Cl^-]$ in methanol (40%) was purchased from Gelest. NPES $[C_9H_{19}C_6H_4O(CH_2CH_2O)_{10}SO_3^-K^+]$ was provided by Aldrich.

B. Preparation of composite-coated separator

A mixture of concentrated HNO_3 and H_2SO_4 in a ratio of 1:3 (V:V) was used to oxidize the CNT at 50 °C for 3 h. The as-prepared suspension was then centrifuged and washed twice with deionized

water. DC5700 and NPES were added in succession to react with the oxidized CNT. The organically modified CNT thus obtained was dried at 70 °C for 24 h in a vacuum oven before use. ZrO_2 (90 wt%) and polyvinylidene fluoride (PVDF) powder (10 wt%) were thoroughly ground in a mortar for about 1 h. The powder mixture was blended with a defined amount of the modified CNT (CNT:ZrO_2 = 2:1, W:W), after which NMP was added to give a slurry that was then thoroughly mixed by magnetic stirring for 4 h to give a consistency suitable for coating. The desired amount of the mixture was then spin-coated onto one surface of a blank separator that had previously been washed with ethanol in an ultrasonic cleaner to remove pollutants. For comparison, one modified separator was prepared with a coating thickness of about 14 μm (CNT/ZrO_2-14) and one with a coating thickness of 18 μm (CNT/ZrO_2-18). For both thicknesses, the mass ratio of CNT/ZrO_2 composite to NMP was 1:1, and the rotational speeds of the spin-coating process were 1000 and 800 rev/min for the 14 and 18 μm coatings, respectively. Finally, the coated separator was dried at 50 °C under vacuum for 24 h. A CNT/MnO_2 composite-coated separator with a coating thickness of 14 μm was prepared by the same procedure for comparison.

C. Characterizations

A scanning electron microscope (SEM) (QUANTA FEG 450) was used to investigate the surface morphologies of the different separators. The pore size and distribution of the CNT/ZrO_2 composites were characterized by the Brunauer–Emmett–Teller (BET) method using an ASAP 2020 instrument. X-ray diffraction (XRD) patterns were obtained with an X-ray diffractometer (RU-200B/D/MAX-RB). Liquid uptake of the separators at different times was measured in a glove box filled with argon according to the following expression:

$$\eta = (W_t - W_0)/W_0 \times 100\%, \tag{1}$$

where W_0 and W_t are the weights of the separator before and after a certain period of immersion in the electrolyte, respectively. A JC 2000C instrument was used to measure the water contact angles of the blank and modified separators. The thermal shrinkages of the different separators were calculated from

$$S = (L_0 - L)/L_0 \times 100\%, \tag{2}$$

where L_0 and L are the machine direction (MD) lengths of the original and thermally treated separators, respectively.

For the purpose of evaluating and comparing the electrochemical performances of the blank and CNT/ZrO_2 composite-coated separators, coin-type (CR2032) batteries were assembled in a glove box under an argon atmosphere. An electrolyte composed of 1 M LiTFSI in a DME/DOL (V/V = 1:1) solution with the addition of 1 wt% $LiNO_3$ was used in the cell. The cathode was made of PVDF, acetylene black, and elemental sulfur in a ratio of 1:2:3 by weight. The sulfur loading of the electrode was around 1.5 mg/cm^2. The amount of electrolyte was determined by the mass of sulfur in each battery. For an electrolyte/sulfur ratio of 10 μL/mg, about 20 μL of electrolyte was added to the battery. A desktop glue machine (KW-4A) was used for spin coating. The thickness of the CNT-coated separator was kept the same as that of the CNT/ZrO_2 composite-coated separator. The anode material was lithium metal foil. The cycling performance of the cell was tested with a LAND CT2001A system. Cyclic voltammetry (CV) was performed with an electrochemical workstation (CHI 660E). The voltage range adopted was 1.5–3 V, with a scanning rate of 0.1 mV/s for CV measurement.

III. RESULTS AND DISCUSSION

Fig. 1(a) shows the blank and CNT/ZrO_2 composite-coated separators. The surface morphologies of the separators as characterized by SEM are shown in Figs. 1(b)–1(d). The blank separator typically exhibits large numbers of slit-like pores. For the CNT/ZrO_2 composite-coated separators of either coating thickness, the surface is covered by a uniform layer of composite in which irregular pore structures can be seen. These miniature pore structures help to increase electrolyte absorption, thereby promoting the migration of ions between the cathode and anode during the charge and discharge process.[14]

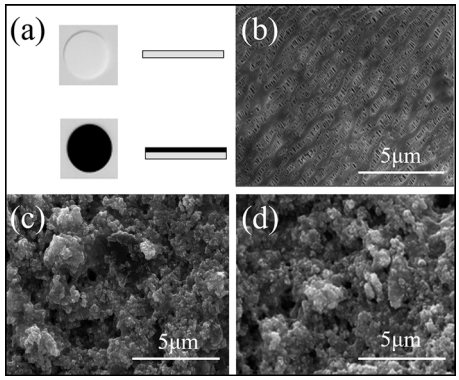

FIG. 1. (a) Photographs of the blank and CNT/ZrO_2 composite-coated separators. (b)–(d) SEM images of the blank separator, the CNT/ZrO_2-14 composite-coated separator, and the CNT/ZrO_2-18 composite-coated separator, respectively.

The type II isotherm in Fig. 2(a) implies the presence of macropores in the CNT/ZrO_2 composites. The pore-size distribution analysis in Fig. 2(b) demonstrates that the pore size is concentrated around 100 nm. According to the results of the BET analysis, the surface area and total pore volume are 190 m^2/g and 0.1 cm^3/g, respectively.

The XRD pattern of the CNT/ZrO_2 composite is shown in Fig. 3. The peaks around 28.0°, 28.3°, 40.5°, 49.2°, and 50.0° correspond to the (1 0 1), (1 1 0), (2 0 0), (1 1 2), and (2 1 1) crystallographic

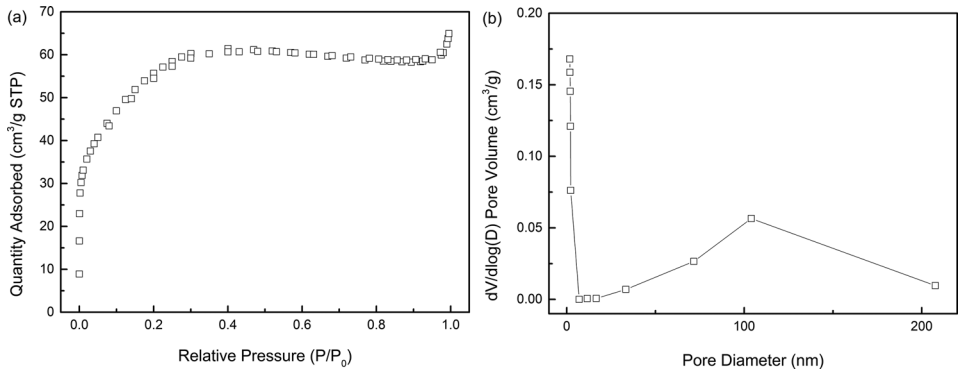

FIG. 2. (a) N_2 sorption isotherm curve and (b) pore-size distribution of the CNT/ZrO_2 composite.

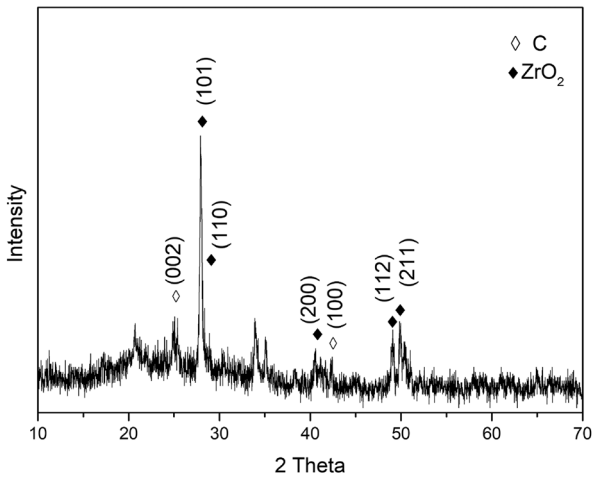

FIG. 3. XRD pattern of the CNT/ZrO_2 composite.

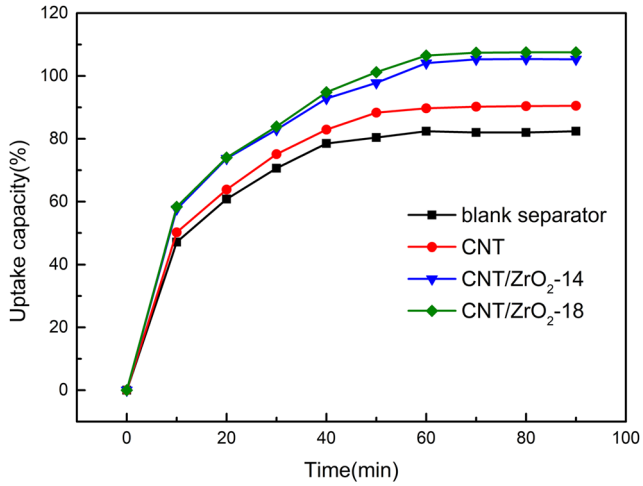

FIG. 4. Liquid uptake capacities of the blank, CNT-coated, and CNT/ZrO_2-14 and CNT/ZrO_2-18 composite-coated separators.

planes, respectively, of ZrO_2, and the peaks at 25° and 42° correspond to the (0 0 2) and (1 0 0) crystallographic planes, respectively, of the CNT. The XRD result confirms that the composite is indeed composed of CNT and ZrO_2.

The liquid uptake capacities of the blank, CNT-coated, and CNT/ZrO_2 composite-coated separators determined using Eq. (1) are shown in Fig. 4. It is clear that the liquid uptake capacities of all the separators initially rose and then leveled out and remained stable after 60 minutes. At all times, the liquid uptakes of the CNT/ZrO_2 composite-coated separators were higher than those of the blank and CNT-coated separators. The blank separator was able to rely only on its internal pore structure to absorb electrolyte, whereas for the composite-coated separators, the plentiful hydrophilic hydroxyl and carboxyl groups and the long-chain organic molecules grafted onto the CNT, together with the pore structures in the composite, could simultaneously absorb and contain the electrolyte, thus enhancing the overall liquid absorption capacity of the separator. The composite-coated separator with a coating thickness of 18 μm showed a slightly greater uptake capacity than the one with a 14 μm coating. The improved electrolyte absorption is believed to promote ionic migration between cathode and anode throughout the charge and discharge process, contributing to optimization of the Li–S battery performance.

Since the surface of a separator must have a good wetting capability, water contact angle (WCA) measurements were performed to determine the polarity of the separators. Figure 5 shows the WCA results for the blank and CNT/ZrO_2 composite-coated separators. It can be seen from Fig. 5(a) that the blank separator has a water contact angle of about 114°, which is consistent with previous results and with the hydrophobic nature of the polypropylene on which the blank separator is based. In contrast, as can be seen from Figs. 5(b) and 5(c), there was almost complete spread of the added water on the composite-coated separator and it was not possible to measure the contact angle.

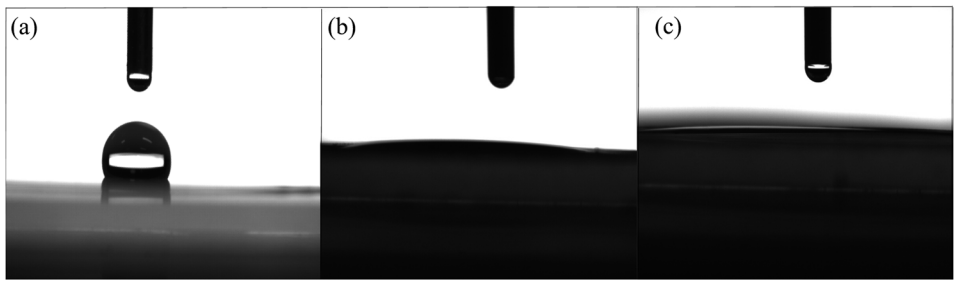

FIG. 5. Water contact angles of (a) the blank separator and (b, c) the CNT/ZrO_2-14 and CNT/ZrO_2-18 composite-coated separators, respectively.

This indicates even greater hydrophilicity than that indicated by the 15° contact angle of the CNT-coated separator.[35] These results provide further evidence of the presence on the surface of the CNT of long-chain organic molecules with plentiful hydrophilic hydroxyl and carboxyl groups. It is well known that hydrophilicity of the side of the separator facing the cathode should help adsorption of polysulfides, thus contributing to suppression of the shuttle effect.[37] In addition, the porous structure of the composite will help to accommodate a greater amount of electrolyte and polysulfides.

Figure 6 shows the percentage of thermal shrinkage calculated from Eq. (2) after the separators were treated for half an hour at various temperatures from 100 to 155 °C. It can be seen that when the temperature reached 155 °C, the shrinkage of the blank separator was as high as 43%, but was only 35% for the CNT-coated separator, and considerably less, only 24%, for the CNT/ZrO_2 composite-coated separators, which shows their excellent thermal dimensional stability. Similar differences in shrinkage can also be seen at lower temperatures. The similarity of the results for the CNT/ZrO_2-14 and CNT/ZrO_2-18 composite-coated separators suggests that the effect of composite thickness was negligible. In addition, the average slope in each temperature interval for the CNT/ZrO_2 composite-coated separators was lower than the slopes for the blank and CNT-coated separators. This suggests that ZrO_2 nanoparticles remain stable and help prevent the disappearance of micropores, thus ensuring the high-temperature stability of the separators. The excellent thermal dimensional stability of the modified separators observed here suggests that they will be of benefit for the practical application of Li–S batteries.

To preclude the possibility that the CNT or ZrO_2 nanoparticles might affect the electrochemical reaction inside the battery, cyclic voltammograms of batteries assembled with the blank and CNT/ZrO_2 composite-coated separators were measured, and the results are shown in Fig. 7. For all the batteries, there are two reduction peaks around 2.3 and 2.0 V in the discharge process and an oxidation peak near 2.5 V in the charge process. According to previous reports, the higher reduction peak represents the conversion of S_8 to soluble long-chain polysulfides (Li_2S_x, x = 4, 6, 8) and the lower peak the generation of Li_2S_2/Li_2S, while the oxidation peak is ascribed to the transition from Li_2S_2/Li_2S to elemental sulfur.[38–40] Compared with the cyclic voltammogram of the blank separator, those of the CNT/ZrO_2 composite-coated separators show the same redox peaks at similar locations, suggesting that neither CNT nor ZrO_2 participates in the electrochemical reaction in the charge and discharge process. The cyclic voltammograms of the CNT/ZrO_2-14 and CNT/ZrO_2-14 composite-coated separators are similar to each other, indicating that the coating thickness did not affect the electrochemical reaction. In addition, the first three cyclic voltammograms in Figs. 7(b) and 7(c) show greater similarity with each other than do those in Fig. 7(a), which indicates that batteries with CNT/ZrO_2 composite-coated separators exhibit a greater degree of reversibility of electrochemical reaction.

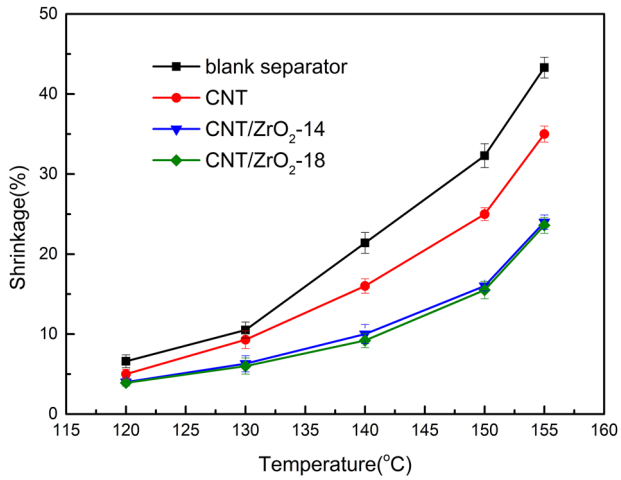

FIG. 6. Thermal shrinkage properties of the blank, CNT-coated, and CNT/ZrO_2-14 and CNT/ZrO_2-18 composite-coated separators.

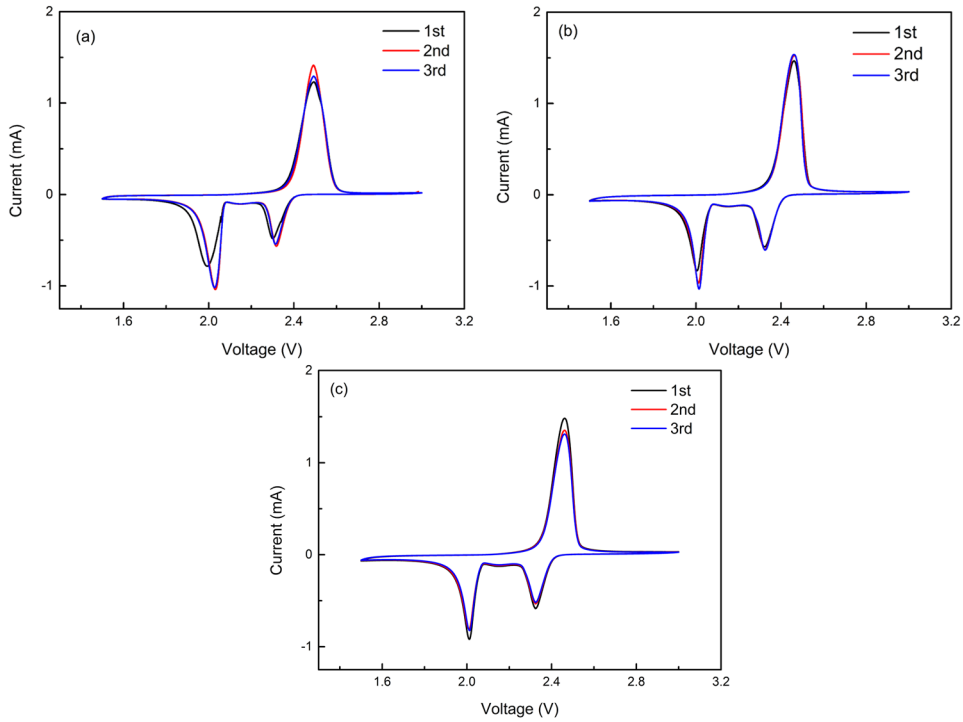

FIG. 7. Cyclic voltammograms of (a) the blank separator and (b, c) the CNT/ZrO_2-14 and CNT/ZrO_2-18 composite-coated separators, respectively.

The cyclic performance of batteries with the blank, CNT-coated, CNT/ZrO_2 composite-coated, and CNT/MnO_2 composite-coated separators at 0.1 C are compared in Fig. 8(a). The batteries with the CNT/ZrO_2 composite-coated separators released an initial capacity of up to 1207 mA·h/g at

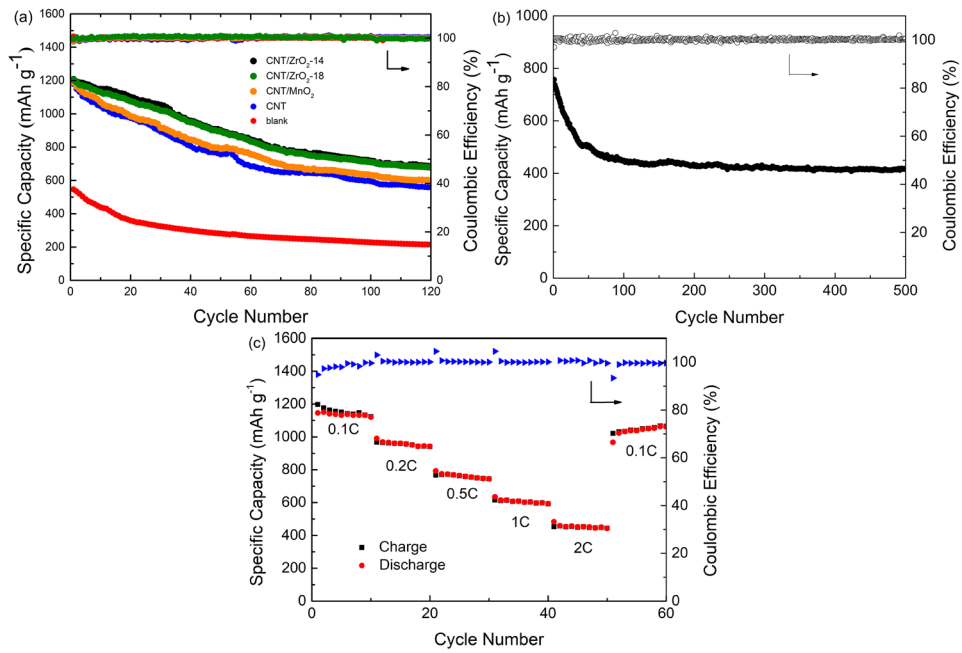

FIG. 8. (a) Cyclic performances of the blank, CNT-coated, and CNT/ZrO_2-14, CNT/ZrO_2-18 and CNT/MnO_2 composite-coated separators at 0.1 C. (b) Cyclic performance of the CNT/ZrO_2-14 composite-coated separator at 1 C. (c) Rate performance of the CNT/ZrO_2-14 composite-coated separator.

0.1 C, whereas the batteries with CNT-coated and blank separators released initial capacities of 1179 and 546 mA·h/g, respectively. Moreover, after 120 cycles, the discharge capacities of the batteries with CNT/ZrO_2 composite-coated separators remained as high as 685 mA·h/g, giving a capacity retention rate of 56.7%, whereas the batteries with CNT-coated or blank separators had rates of only 47.5% and 39.3%, respectively. Thus, the use of CNT/ZrO_2 composite-coated separators improves the initial discharge capacity compared with CNT-coated and blank separators. It should be noted that this improvement in capacity retention rate is of great importance for practical application of batteries.

The increased capacity retention rate seems to be due to the effect of the CNT/ZrO_2 composite coating layer, which traps long-chain polysulfides and accommodates a greater amount of electrolyte during cycling.[35,41] The separators with CNT/ZrO_2-14 and CNT/ZrO_2-18 composite coatings exhibited similar cycling performances to each other, and so it appears that increasing the coating thickness will not improve the cycling performance. On the other hand, the thickness of the composite layer could affect the volumetric energy density of the battery. That is to say, for a given battery energy, the greater the coating thickness, the lower is the energy density. With this in mind, the coating should be as thin as the process conditions permit. It should be noted that the cyclic performance of the CNT/MnO_2 composite-coated separator was similar to that of the CNT-coated separator, indicating the superiority of ZrO_2 when used in the composite.

Figure 8(b) shows the high-current-rate cyclic performance of the battery with a CNT/ZrO_2-14 composite-coated separator at 1 C. The reversible capacity in 500 cycles decreases from 757 to 417 mA·h/g, while the capacity retention rate reaches 55% and the coulombic efficiency about 99%. This encouraging result shows that the structure of the CNT/ZrO_2 coating on the separator retained its stability and ensured ionic migration in the system. In other words, even rapid reactions will not cause the structure to collapse during the charge and discharge process, giving the Li–S battery a long cycle life at high current.

The battery with a CNT/ZrO_2-14 composite-coated separator also exhibited a good rate performance. Figure 8(c) shows that the discharge capacity rose to 1145 mA·h/g at 0.1 C in the first cycle, and remained near 960, 750, 610, and 450 mA·h/g at 0.2, 0.5,1, and 2 C, respectively, in 10 cycles, and it still reached 1050 mA·h/g even once the current rate returned to 0.1 C. The impressive reversibility of the capacity of up to 91.7% confirms the excellent reversibility and stability of the Li–S battery with a CNT/ZrO_2 composite-coated separator.

IV. CONCLUSIONS

We have adopted a CNT/ZrO_2 composite as a coating layer on the separator in a Li–S battery and have thereby effectively improved its electrochemical performance and thermal shrinkage properties. The pore structure formed by organically modified CNT and ZrO_2 nanoparticles is able to accommodate a greater amount of electrolyte and help ionic migration during the process of charge and discharge. The addition of ZrO_2 increases the thermal dimensional stability of the separator. The use of the CNT/ZrO_2 composite improves electrochemical performance by suppressing the shuttle effect. Thus, the improvements achieved by the strategy adopted here of modifying the separator in Li–S batteries makes these promising candidates for commercial production.

ACKNOWLEDGMENTS

Financial support from the National Science Foundation of China (Grant No. 51673154) is gratefully acknowledged.

[1] J.-M. Tarascon and M. Armand, Nature **414**, 359 (2001).
[2] P. G. Bruce, B. Scrosati, and J.-M. Tarascon, Angew. Chem. Int. Ed. **47**, 2930 (2008).
[3] J. Kaspar, M. Graczyk-Zajac, S. Choudhury, and R. Riedel, Electrochim. Acta **216**, 196 (2016).
[4] S. K. Srivastava, B. Kartick, S. Choudhury, and M. Stamm, Mater. Chem. Phys. **183**, 383 (2016).
[5] M. S. Whittingham, Chem. Rev. **114**, 11414 (2014).
[6] S. Evers and L. F. Nazar, Acc. Chem. Res. **46**, 1135 (2013).
[7] Z. W. Seh, Y. Sun, Q. Zhang, and Y. Cui, Chem. Soc. Rev. **45**, 5605 (2016).
[8] X. Ji and L. F. Nazar, J. Mater. Chem. **20**, 9821 (2010).
[9] A. Manthiram, S.-H. Chung, and C. Zu, Adv. Mater. **27**, 1980 (2015).

[10] S. Choudhury, B. Krüner, P. Massuti-Ballester, A. Tolosa, C. Prehal, I. Grobelsek, O. Paris, L. Borchardt, and V. Presser, J. Power Sources **357**, 198 (2017).
[11] I. Gomez, D. Mecerreyes, J. A. Blazquez, O. Leonet, H. Ben Youcef, C. Li, J. L. Gómez-Cámer, O. Bondarchuk, and L. Rodriguez-Martinez, J. Power Sources **329**, 72 (2016).
[12] S. Choudhury, P. Srimuk, K. Raju, A. Tolosa, S. Fleischmann, M. Zeiger, K. I. Ozoemena, L. Borchardt, and V. Presser, Sustainable Energy & Fuels **2**, 133 (2018).
[13] S. Choudhury, M. Agrawal, P. Formanek, D. Jehnichen, D. Fischer, B. Krause, V. Albrecht, M. Stamm, and L. Ionov, ACS Nano **9**, 6147 (2015).
[14] Z. Zhang, Y. Lai, Z. Zhang, K. Zhang, and J. Li, Electrochim. Acta **129**, 55 (2014).
[15] Y. Fu, Y. S. Su, and A. Manthiram, Angew. Chem. Int. Ed. **125**, 7068 (2013).
[16] J. Cao, C. Chen, Q. Zhao, N. Zhang, Q. Lu, X. Wang, Z. Niu, and J. Chen, Adv. Mater. **28**, 9629 (2016).
[17] R. C. Chen, T. Zhao, T. Tian, S. Cao, P. R. Coxon, K. Xi, D. Fairen-Jimenez, R. V. Kumar, and A. K. Cheetham, APL Mater. **2**, 124109 (2014).
[18] J. S. Lee, J. Jun, J. Jang, and A. Manthiram, Small **13**, 1062984 (2017).
[19] Q. Pang, D. Kundu, M. Cuisinier, and L. F. Nazar, Nat. Commun. **5**, 4759 (2014).
[20] Y. Zhou, C. Zhou, Q. Li, C. Yan, B. Han, K. Xia, Q. Gao, and J. Wu, Adv. Mater. **27**, 3774 (2015).
[21] Z. Tang, Q. Yang, B. Liu, M. Wang, S. Wang, and C. Xiong, Macromol. Mater. Eng. **302**, 1700122 (2017).
[22] W. Li, Q. Zhang, G. Zheng, Z. W. Seh, H. Yao, and Y. Cui, Nano Lett. **13**, 5534 (2013).
[23] R. Song, R. Fang, L. Wen, Y. Shi, S. Wang, and F. Li, J. Power Sources **301**, 179 (2016).
[24] H. Yao, K. Yan, W. Li, G. Zheng, D. Kong, Z. W. Seh, V. K. Narasimhan, Z. Liang, and Y. Cui, Energy Environ. Sci. **7**, 3381 (2014).
[25] H.-J. Peng, D.-W. Wang, J.-Q. Huang, X.-B. Cheng, Z. Yuan, F. Wei, and Q. Zhang, Adv. Sci. **3**, 1500268 (2016).
[26] L. Wang, J. Liu, S. Haller, Y. Wang, and Y. Xia, Chem. Commun. **51**, 6996 (2015).
[27] J. Zhu, M. Yanilmaz, K. Fu, C. Chen, Y. Lu, Y. Ge, D. Kim, and X. Zhang, J. Membr. Sci. **504**, 89 (2016).
[28] I. Bauer, S. Thieme, J. Brückner, H. Althues, and S. Kaskel, J. Power Sources **251**, 417 (2014).
[29] S. Choudhury, M. Azizi, I. Raguzin, M. Gobel, S. Michel, F. Simon, A. Willomitzer, V. Mechtcherine, M. Stamm, and L. Ionov, Phys. Chem. Chem. Phys. **19**, 11239 (2017).
[30] S.-H. Chung and A. Manthiram, Adv. Funct. Mater. **24**, 5299 (2014).
[31] S. S. Zhang, J. Power Sources **164**, 351 (2007).
[32] H. Pan, Z. Cheng, Z. Xiao, X. Li, and R. Wang, Adv. Funct. Mater. **27**, 1703936 (2017).
[33] C. Xu, H. Zhou, C. Fu, Y. Huang, L. Chen, L. Yang, and Y. Kuang, Electrochim. Acta **232**, 156 (2017).
[34] S. H. Chung and A. Manthiram, J. Phys. Chem. Lett. **5**, 1978 (2014).
[35] B. Liu, X. Wu, S. Wang, Z. Tang, Q. Yang, G.-H. Hu, and C. Xiong, Nanomaterials **7**, 196 (2017).
[36] S. M. Lee, S. H. Oh, J. P. Ahn, W. I. Cho, and H. Jang, J. Power Sources **159**, 1334 (2006).
[37] C. Zu, Y. S. Su, Y. Fu, and A. Manthiram, Phys. Chem. Chem. Phys. **15**, 2291 (2013).
[38] F. Wu, J. Chen, R. Chen, S. Wu, L. Li, S. Chen, and T. Zhao, J. Phys. Chem. C **115**, 6057 (2011).
[39] J. Sun, Y. Huang, W. Wang, Z. Yu, A. Wang, and K. Yuan, Electrochim. Acta **53**, 7084 (2008).
[40] J.-W. Choi, G. Cheruvally, D.-S. Kim, J.-H. Ahn, K.-W. Kim, and H.-J. Ahn, J. Power Sources **183**, 441 (2008).
[41] C. Wan, W. Wu, C. Wu, J. Xu, and L. Guan, RSC Adv. **5**, 5102 (2015).